

Analysis of the *Xenopus* Werner syndrome protein in DNA double-strand break repair

Hong Yan, Jill McCane, Thomas Toczylowski, and Chinyi Chen

Fox Chase Cancer Center, Philadelphia, PA 19111

Werner syndrome is associated with premature aging and increased risk of cancer. Werner syndrome protein (WRN) is a RecQ-type DNA helicase, which seems to participate in DNA replication, double-strand break (DSB) repair, and telomere maintenance; however, its exact function remains elusive. Using *Xenopus* egg extracts as the model system, we found that *Xenopus* WRN (xWRN) is recruited to discrete foci upon induction of DSBs. Depletion of xWRN

has no significant effect on nonhomologous end-joining of DSB ends, but it causes a significant reduction in the homology-dependent single-strand annealing DSB repair pathway. These results provide the first direct biochemical evidence that links WRN to a specific DSB repair pathway. The assay for single-strand annealing that was developed in this study also provides a powerful biochemical system for mechanistic analysis of homology-dependent DSB repair.

Introduction

Werner syndrome (WS) is a rare genetic disorder that causes the premature development of a variety of age-related diseases, such as arteriosclerosis, diabetes, osteoporosis, graying and loss of hair, and skin degeneration (Schellenberg et al., 1998). In addition, ~10% of affected individuals develop tumors, mostly of mesenchymal origin. The median age of death for patients who have WS is 47 yr; the major causes of death are coronary artery atherosclerosis and cancer. At the cellular level, WS fibroblast cells have markedly reduced replicative life spans compared with age-matched controls (Martin et al., 1970; Salk et al., 1981). They exhibit elevated rates of chromosomal rearrangements (Hoehn et al., 1975; Salk et al., 1981; Scappaticci et al., 1982). The rate of somatic mutations is also increased, and most of the mutations appear to be deletions of large segments of DNA (>20 kb) (Fukuchi et al., 1989; 1990). The genome instability in WS cells is likely to be the driving force for premature aging and cancer in patients who have WS.

The gene that is deficient in WS (*WRN*) encodes a member of the RecQ DNA helicase family (Yu et al., 1996). Unlike other members, Werner syndrome protein (WRN) also contains an exonuclease domain that is similar to the proofreading exonuclease domain of *Escherichia coli* DNA polymerase I

(Mushegian et al., 1997). Mutations in WRN and other RecQ helicases cause defects in DNA replication, DNA double-strand break (DSB) repair, homologous recombination (HR), telomere maintenance, and apoptosis (Shen and Loeb, 2000; Khakhar et al., 2003; Comai and Li, 2004; Lee et al., 2005). At the mechanistic level, the major function for WRN seems to be the promotion of replication fork restart and DSB repair. WS cells display various defects in replication, such as fewer initiation events for replication (Takeuchi et al., 1982a; Hanaoka et al., 1983), misfiring of origins (Fujiwara et al., 1985), reduced DNA chain-elongation rates (Fujiwara et al., 1977), a prolonged S phase (Takeuchi et al., 1982b), asymmetric replication forks (Rodriguez-Lopez et al., 2002), and lagging strand DNA synthesis of telomeres (Crabbe et al., 2004). The current model suggests that WRN (and other RecQ helicases) facilitate the restart of stalled replication forks. Replication forks frequently stall or collapse in bacteria (Cox et al., 2000) and eukaryotes (Lopes et al., 2001). These roadblocks can take many forms, such as nicks, lesions, sequences that can form secondary structures (i.e., telomere repeats), and tightly bound proteins. After stalling, the two newly synthesized strands are dissociated from parental templates and annealed with each other, which lead to the formation of a chicken-foot structure (pseudo-Holliday junction) (McGlynn et al., 2001; Postow et al., 2001). WRN can unwind Holliday junctions in vitro, and it has been proposed to facilitate replication restart by reversing the chicken-foot structure (Constantinou et al., 2000). This model provides an elegant explanation of WRN's role in replication, but it has not been tested rigorously.

Correspondence to Hong Yan: Hong_Yan@fccc.edu

Abbreviations used in this paper: DSB, double-strand break; HR, homologous recombination; NHEJ, nonhomologous end joining; NPE, nucleoplasmic extract; SSA, single-strand annealing; *Tet*, tetracycline resistance gene; WRN, Werner syndrome protein; WS, Werner syndrome; xWRN, *Xenopus* WRN.

The online version of this paper contains supplemental material.

In addition to replication, there is evidence that WRN participates in DNA DSB repair. DNA DSBs are the most deleterious type of DNA damage in cells. It was estimated that up to 50 DSBs are produced during each cell cycle, most of which probably are the result of replication forks that encounter lesions or nicks in template DNA (Vilenchik and Knudson, 2003). Three major pathways have been identified to repair DSBs in eukaryotic cells: nonhomologous end joining (NHEJ), HR, and single-strand annealing (SSA) (Baumann and West, 1998). In NHEJ, DNA ends are processed and then ligated directly, as such, this pathway is intrinsically error-prone. In HR, DNA ends are processed into 3' single-strand (ss) tails, which then invade a homologous sequence and copy the missing information. SSA occurs when the break lies between two direct repeats. Each repeat is processed into single strands, which are then annealed and ligated, with one of the repeats effectively deleted. Like HR, SSA is homology dependent, and both pathways are initiated by the processing of broken DNA ends into ss-tails. Moreover, recent genetic studies in yeast and *Drosophila* suggested that HR and SSA share additional mechanistic similarities (Symington, 2002). Although meiotic HR proceeds by way of Holliday junction formation and resolution, mitotic HR seems to use synthesis-dependent DNA annealing during which the invading strand is extended but then released from the D-loop before the formation of Holliday junction structure. This extended strand is complementary to the processed single strand from the other side, and the break is then repaired in a reaction that is essentially identical to SSA.

Several lines of evidence suggest that WRN has a role in DSB repair. WS cells are defective in homology-based recombination (Prince et al., 2001), the WRN protein interacts with NHEJ protein Ku (Cooper et al., 2000; Li and Comai, 2000), and linear DNA introduced into WS cells suffers more extensive deletions at the ends (Oshima et al., 2002). However, it is unclear if WRN is involved directly or indirectly in these repair pathways—and if directly—what mechanistic

role it plays. To address these important issues, we initiated a biochemical study of WRN's function in DSB repair by using *Xenopus* egg extracts as the model system. This system can reconstitute DNA replication (Lohka and Masui, 1983; Newport, 1987), and efficiently joins pairs of DNA ends bearing 5' protruding single strands (PSS), 3' PSS, and blunt ends with high efficiency and precision (Thode et al., 1990). The repair is Ku dependent, which suggests that it is mediated by a bona fide NHEJ reaction (Labhart, 1999). The other two DSB repair pathways, HR and SSA, have not been reconstituted in *Xenopus* egg extracts. However, a series of studies showed that linear DNA containing direct repeats on each end can be repaired by SSA when injected into oocytes or unfertilized eggs, or when incubated in extracts that were derived from germinal vesicles of oocytes (Carroll, 1996). As was shown in this study, SSA also can be reconstituted efficiently in nucleoplasmic extracts (NPEs) that were derived from nuclei reconstituted in *Xenopus* egg extracts. Thus, the *Xenopus* system is ideal for biochemical analysis of NHEJ and homology-dependent repair.

In this study, we found that *Xenopus* WRN (xWRN) is recruited to discrete foci on chromatin in response to DSBs. Depletion of xWRN has no significant effect on the overall efficiency or accuracy of NHEJ repair. However, it causes a significant reduction in the SSA repair pathway. These results provide the first direct biochemical evidence to link WRN with a particular DSB repair pathway. The *in vitro* SSA assay that was established in this study also provides an excellent biochemical system for mechanistic analysis of homology-dependent DSB repair.

Results

xWRN is recruited to DSB foci

Many proteins that are involved in DSB repair are recruited to discrete subnuclear foci at the site of damage (Lisby et al.,

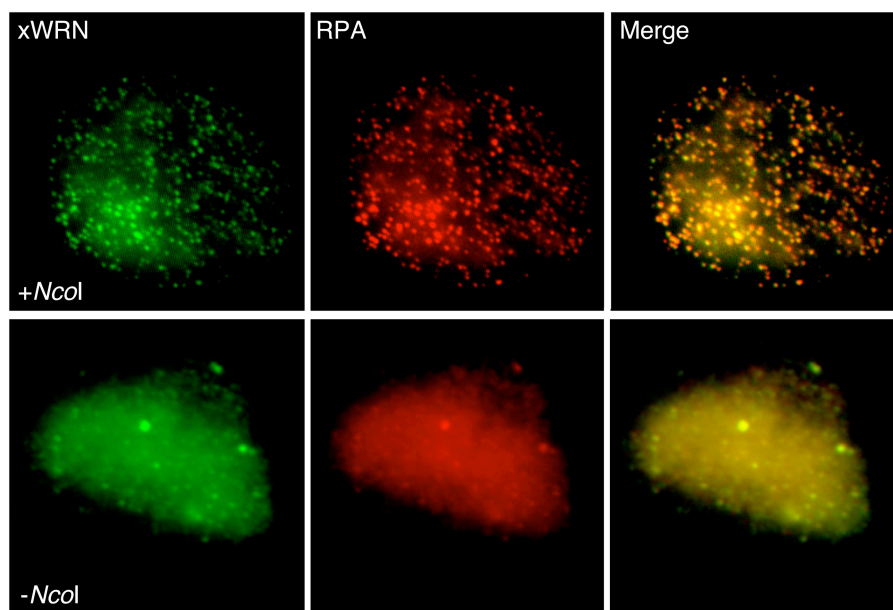


Figure 1. xWRN is recruited to DSB foci. Top: DSBs induce the formation of discrete foci that contain xWRN and RPA. Nuclei were reconstituted in cytosol and membrane fractions in the presence of *NcoI* (+*NcoI*; 0.25 unit/ μ l) or buffer (–*NcoI*). After 60 min, nuclei were fixed and costained with affinity-purified rabbit anti-xWRN and rat anti-RPA followed by goat anti-rabbit FITC and goat anti-rat Texas Red.

2004). It was reported that human WRN is recruited to discrete foci in cells that are treated with various DNA damaging agents, but the agents that were used caused a variety of damages and it is unclear what type of DNA lesion actually triggers the formation of WRN foci (Sakamoto et al., 2001; Blander et al., 2002). To determine definitively if xWRN is recruited to DSB foci, we used restriction enzymes to introduce DSBs into chromatin. In brief, nuclei were reconstituted in the presence of *NcoI* (0.25 unit/ μ l) or buffer, incubated for 60 min, and then fixed and stained with antibodies. As shown in Fig. 1 (top panel), in the presence of *NcoI*, a large number of discrete foci containing xWRN and the eukaryotic single-strand DNA binding protein RPA were formed in the nuclei. Consistent with observations by other investigators (Grandi et al., 2001; Kobayashi et al., 2002), there is very little DNA synthesis in these nuclei because of the activation of checkpoint response that blocks DNA replication (unpublished data). In contrast, in the absence of *NcoI*, xWRN and RPA have a more granular staining pattern (Fig. 1, bottom panel). As reported earlier, this pattern coincides with extensive DNA replication at this time (Chen et al., 2001). In addition to *NcoI*, which generates 5'-protruding ends, restriction enzymes that generate 3'-protruding ends (*KpnI*) or blunt ends (*StuI*) were effective in inducing the formation of DSB foci (unpublished data). RPA was shown to be localized to sequences near DNA ends (Grandi et al., 2001), and physically interacts with xWRN and stimulates its helicase activity (Chen et al., 2001). These observations suggest that xWRN is part of foci formed at

DNA ends. Additional staining with antibodies against replication initiation protein CDC45 (Mimura and Takisawa, 1998; Walter and Newport, 2000) and double-strand DNA end binding protein Ku (Labhart, 1999) showed that DSB foci are distinct from replication foci that are formed in normally reconstituted nuclei. Whereas DSB foci contain Ku, but not CDC45, replication foci contain CDC45, but not Ku (unpublished data). Together these observations are consistent with the notion that xWRN plays dual roles in DSB repair and replication.

xWRN is not important for NHEJ

We then investigated if xWRN is important for the NHEJ pathway of DSB repair. *Xenopus* egg extracts contain robust NHEJ activity that can repair a variety of DNA ends (Pfeiffer and Vielmetter, 1988; Labhart, 1999). We depleted xWRN from cytosol to an undetectable level (>97%; Fig. 2 A) following a procedure that was described before (Chen et al., 2001). The depleted cytosol was incubated with linear pUC19 DNA carrying three different combinations of ends: 5'/blunt (*BamHI/HincII*), 3'/blunt (*KpnI/HincII*), and 5'/3' (*BamHI/PstI*). As shown in Fig. 2 B, repair products corresponding to supercoiled (I) and nicked circular (II) pUC19, as well as linear dimers and trimers, were formed readily after incubation. Compared with mock depletion, xWRN depletion had no significant effect on the formation of these products.

We also determined the effect of xWRN on the accuracy of repair. To do this, the repaired DNA was purified and used

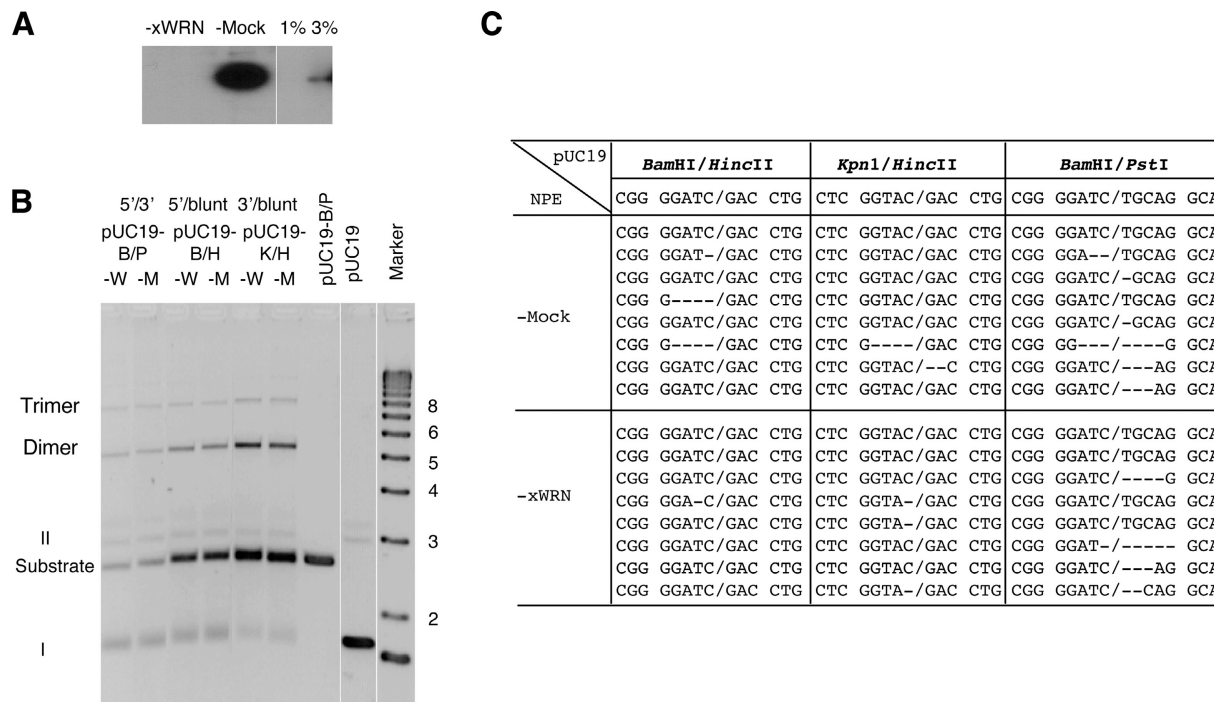


Figure 2. **Depletion of xWRN does not affect NHEJ.** (A) Depletion of xWRN from cytosol. XWRN- or mock-depleted cytosol was loaded on a 7% SDS-PAGE, transferred to an Immobilon P membrane, and probed with the purified rabbit anti-xWRN antibodies. The two lanes on the right are quantitation controls and contain normal cytosol at 1% and 3% of the amount loaded in the lanes containing the depleted cytosol. (B) Linear pUC19 molecules (5 ng/ μ l for -B/P and 10 ng/ μ l for -B/H and -K/H) with different ends were incubated in xWRN-depleted or mock-depleted cytosol at room temperature for 2 h. Samples were treated with SDS/proteinase K, and separated on a 1% agarose gel. Substrates: pUC19-B/P: pUC19 digested by *BamHI* and *PstI*; pUC19-B/H: pUC19 digested by *BamHI* and *HincII*; pUC19-K/H: pUC19 digested by *KpnI* and *HincII*. -W: xWRN-depleted; -M: mock-depleted. (C) Junction sequences of the repaired products. The predicted sequences of perfectly repaired junctions are listed at the top.

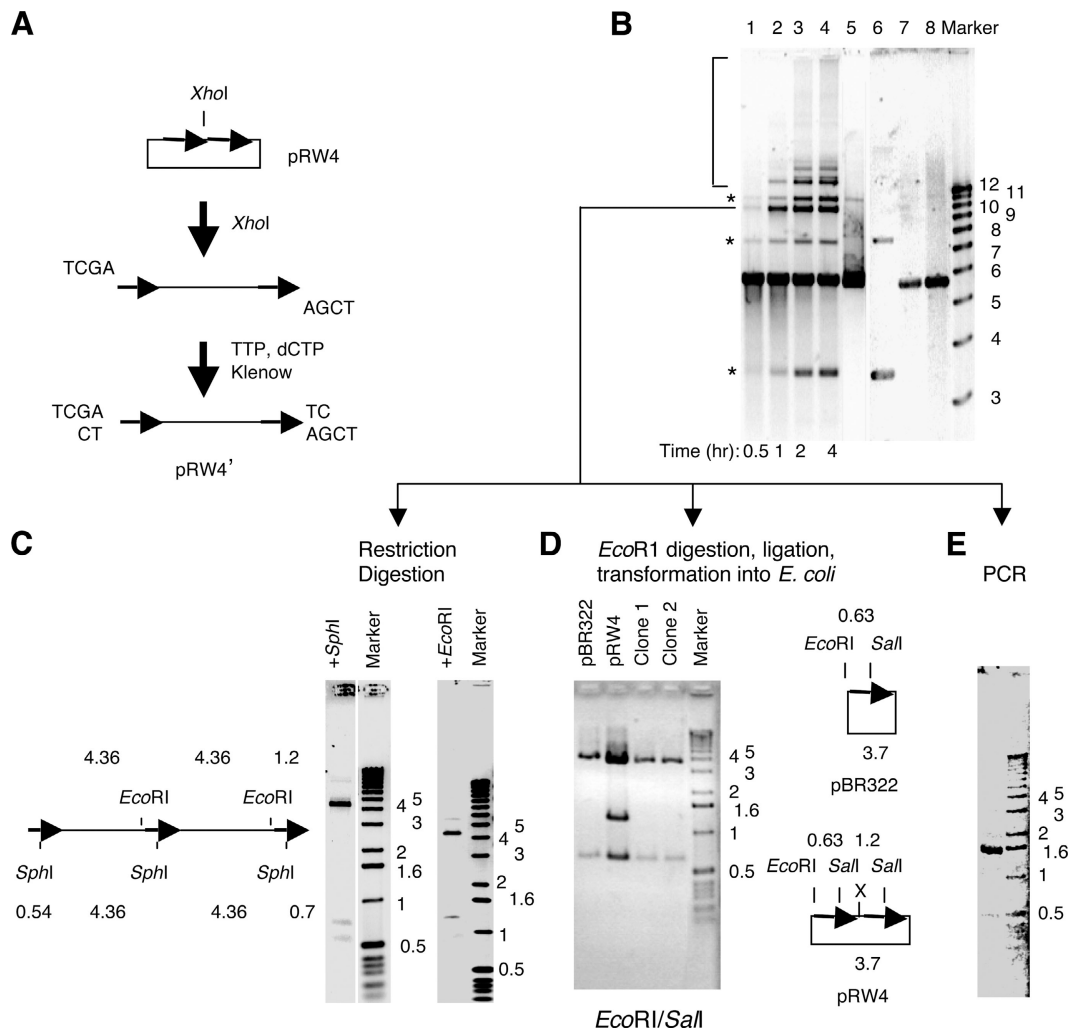


Figure 3. **Establishment of SSA in NPE.** (A) Preparation of the SSA substrate pRW4'. Plasmid pRW4 was digested with *XhoI* and then partially filled in by TTP and dCTP with Klenow (exo; NEB, NE). (B) pRW4' (12 ng/ μ l) was incubated in NPE at room temperature. Samples were taken at the indicated times, treated with SDS/proteinase K, and separated on a 1% agarose gel. Lanes 1–4: time points of the reaction in NPE; lane 5: *XhoI*-digested pRW4 ligated with T4 DNA ligase; lane 6: uncut pRW4; lane 7: pRW4'; lane 8: pRW4' ligated with T4 DNA ligase. Bands indicated by (*) are NHEJ products. (C) Restriction digestion of the 10-kb repair product (indicated by the line in B). Left: predicted digestion pattern by *SalI* and *EcoRI*; middle and right: gel electrophoresis of the digested DNA. The faint bands above the 4.36 band are due to partial digestion. (D) Restriction digestion of the cloned *EcoRI* fragment. Left: gel electrophoresis of the digested plasmid; right: predicted digestion patterns of the pBR322 plasmid and pRW4 plasmid. X: *XhoI* site. (E) Gel electrophoresis of the junction DNA directly amplified from the 10-kb repair product.

for transformation of *E. coli*. Plasmid DNA from individual colonies was isolated and the junctions were sequenced. As shown in Fig. 2 C, repair was very accurate overall, which was consistent with previous observations (Pfeiffer and Vielmetter, 1988; Labhart, 1999). Some mistakes, usually small deletions of a few base pairs, did occur, especially for the 5'/3' end combination. However, there was no significant difference in repair accuracy between the reactions in xWRN-depleted cytosol and mock-depleted cytosol (Fig. 2 C). These results suggest that xWRN is not essential for the efficiency or accuracy of NHEJ repair in *Xenopus* egg extracts.

Establishment of an in vitro SSA assay in NPE

DSBs also can be repaired by two homology-dependent pathways: HR and SSA. Our attempt to establish an HR assay in

Xenopus egg extracts was unsuccessful, but we did succeed in establishing a robust SSA assay. Previously, Carroll (1996) demonstrated that SSA can occur after DNA is injected into oocytes or unfertilized eggs or after it is incubated in germinal vesicle extracts. However, the injection method is incompatible with immunodepletion, and germinal vesicle extracts seem to be too dilute to survive immunodepletion. The assay that we established uses NPE, which is derived from nuclei reconstituted in *Xenopus* egg extracts (Walter et al., 1998). NPE contains high concentrations of nuclear proteins that can catalyze the replication of plasmid DNA. Similarly, we observed that NPE (but not total egg extracts nor membrane-free cytosol) contains robust activity for SSA. The DNA substrate for SSA is a 5.6-kb linearized plasmid, pRW4' (with the *XhoI* ends partially filled in by dCTP and TTP to prevent simple religation), which carries two 1.2-kb direct repeats (tetracycline resistance

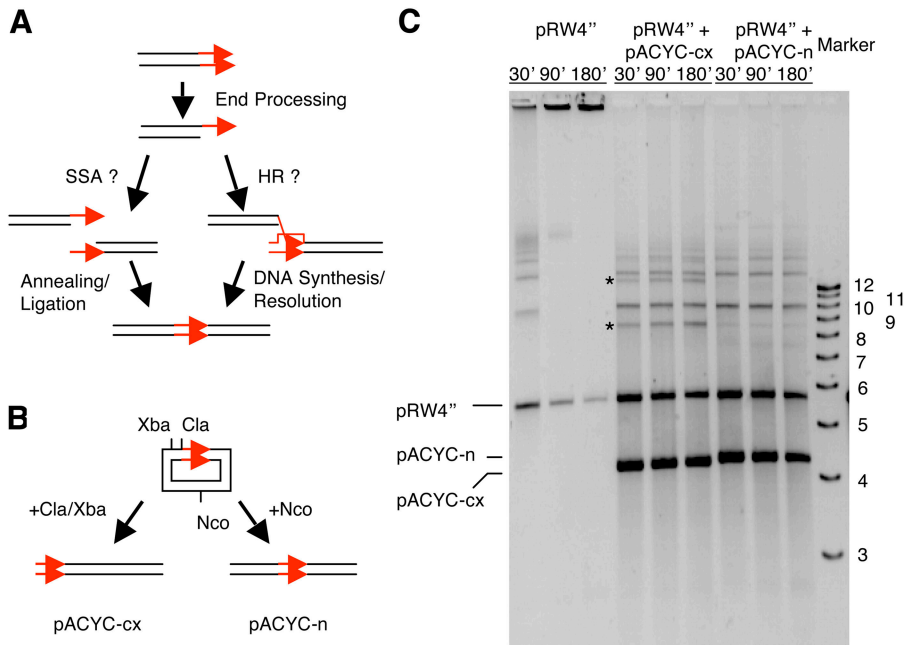


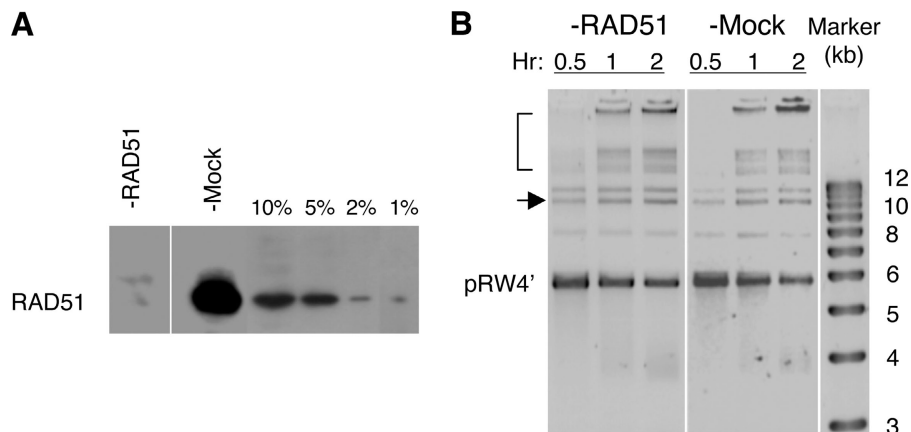
Figure 4. Distinction between SSA and HR. (A) Two potential pathways for generating the 10-kb repair product. SSA uses ss-tail for annealing with the complementary ss-tail, whereas HR uses the ss-tail for invasion of ds-DNA to form a D-loop. (B) Substrates used to distinguish between SSA and HR. Digestion by *ClaI* and *XbaI* generates pACYC-c/x and places the Tet gene at the end. Digestion by *NcoI* generates pACYC-n and places the Tet gene in the middle. (C) Gel electrophoresis of the repair products after DNA substrates (12 ng/ μ l each) were incubated in NPE at room temperature for the indicated times. All three DNA substrates were extended with TTP, dATP, dCTP, and ddGTP. pRW4'' is different from pRW4' in that it contains an extra ddGTP at the end. Bands indicated by (*) are hybrid repair products formed between pRW4'' and pACYC-cx.

gene; *Tet*) at the two ends (Fig. 3 A) (Maryon and Carroll, 1989). As shown in Fig. 3 B (lanes 1–4), after incubation in NPE, pRW4' was converted into multiple products. Three of the bands (*) correspond to supercoiled circular monomer, nicked circular monomer, and linear dimer of pRW4'. They were not formed by simple religation, because the ends are not complementary (compare with lane 8). In addition to these three bands, we detected a prominent 10-kb band (and many higher molecular weight bands that were produced even when NHEJ was inhibited [see Fig. 4 C]). The size of the 10-kb band was consistent with the expected size of an intermolecular SSA reaction product. When this band was isolated from gel, its restriction digestion pattern was that expected of the SSA product (Fig. 3 C). The junction DNA was cloned by ligating the *EcoRI*-digested DNA with T4 ligase, followed by transformation into *E. coli*. The transformants were resistant to ampicillin and—when restreaked—to tetracycline (16/16; DNA not treated with T4 DNA ligase did not give rise to transformants). The plasmids that were isolated from the transformants were analyzed by restriction digestion and were found to have the same pattern as that of pBR322, the parent plasmid of pRW4' (6/6; two shown in Fig. 3 D). Sequence analysis confirmed that the junction sequence in the clones is the same as the sequence around the *Tet* gene in pBR322 (Fig. S1; available at <http://www.jcb.org/cgi/content/full/jcb.200502077/DC1>). Furthermore, PCR amplification of the 10-kb repair product with two primers that bracket the *Tet* repeat gave rise to a 1.5-kb product as predicted from SSA (Fig. 3 E). Direct sequencing of this PCR product showed that it also is the same as the *Tet* gene in pBR322 (Fig. S2). Of particular importance is that the *XhoI* site between the two *Tet* repeats in pRW4 is missing in the cloned junction and the PCR-amplified junction (Figs. S1 and S2). Taken together, these results strongly suggest that the 10-kb DNA is composed of two linear pRW4 molecules linked in tandem, but with only one *Tet* repeat retained in between.

Distinction between SSA and HR: effect of repeat location

In principle, the 10-kb product can be produced by SSA or HR (Fig. 4 A). Two experiments were conducted to differentiate between these two potential pathways. In the first experiment, we took advantage of the observation that the 10-kb product is generated by an intermolecular reaction. A different plasmid, pACYC184, which has no significant sequence homology to pRW4 except in the *Tet* gene, was linearized by digestion with different restriction enzymes (Fig. 4 B). Double digestion by *ClaI* and *XbaI* placed *Tet* at one end of the linear molecule (pACYC-cx), whereas single digestion by *NcoI* digestion placed *Tet* in the middle (pACYC-n). Each DNA was co-incubated with linear pRW4'' (with the *XhoI* ends partially filled in by dCTP, TTP, and ddGTP) in NPE. SSA requires the two repeats to be at ends, but strand invasion, which is the hallmark reaction of HR, should be insensitive to the location of *Tet*. The ends of all three DNA substrates were extended with TTP, dCTP, dATP, and ddGTP to block simple religation and NHEJ (Thode et al., 1990) (Fig. 4 C, lanes 1–3). In the absence of NHEJ, SSA became so efficient that the substrate DNA eventually was converted into products that were too large to enter the gel (Fig. 4 C, lanes 2 and 3). With pACYC-cx, an 8.6-kb product was formed that was consistent with a product between one pRW4 and one pACYC-cx, but with only one *Tet* at the junction (the extra band just below the trimeric pRW4 band is consistent with a product from two pRW4s and one pACYC-cx, but only one *Tet* retained at each junction). In contrast, pACYC-n was inefficient in reacting with pRW4 because no hybrid pRW4–pACYC-n molecules were detected (expected size \sim 7.4 kb). pACYC-cx and pACYC-n interfered with the efficiency of pRW4'' repair because the formation of large repair products was much reduced (compare lanes 1–3 with 4–9). One likely explanation for this interference is that these molecules were still juxtaposed frequently to pRW4'' in

Figure 5. **Effect of xRAD51.** (A) Western blot of the xRAD51- or mock-depleted NPE. The four lanes on the right are quantitation controls and contain normal NPE at 10%, 5%, 2%, and 1% of the amount loaded in the depleted NPE. (B) SSA assay with xRAD51-depleted and mock-depleted NPE. The substrate (pRW4') was incubated in NPE for the indicated times, treated with SDS/proteinase K, and separated by agarose gel electrophoresis. The SSA products include the band indicated by the arrow and a subset of the bands indicated by the bracket.



an attempt at repair. In the case of pACYC-cx, it was combined with pRW4'' by way of SSA, but the resulting product lacked a repeat at the end and further addition of molecules was terminated. In the case of pACYC-n, the attempt to repair between pACYC-n and pRW4'' was futile, but it prevented a pRW4'' molecule from combining with another pRW4'' by way of SSA. Regardless of the exact mechanism for interference, this experiment strongly suggests that the non-NHEJ repair reaction in NPE depends on homology, and that the homology has to be at the ends.

Distinction between SSA and HR: effect of xRAD51

The second experiment that we did to distinguish SSA and HR was to examine RAD51 dependence. RAD51 is the mediator

protein for strand invasion and is essential for D-loop formation during HR. SSA does not involve strand invasion, and genetic studies in *Saccharomyces cerevisiae* showed that it is independent of RAD51 (Ivanov et al., 1996). We depleted xRAD51 from NPE with purified anti-xRAD51 antibodies to at least >99% completion (Fig. 5 A). The xRAD51- and mock-depleted NPEs were incubated with linear pRW4 (pRW4') as described in Fig. 3, and the repair products were separated by agarose gel electrophoresis. As shown in Fig. 5 B, there was no significant difference in the formation of repair products between the xRAD51-depleted and mock-depleted NPEs. Together, this result (independence of RAD51) and the previous result (dependence on homology at ends) strongly suggest that the homology-based repair in NPE is SSA rather than HR.

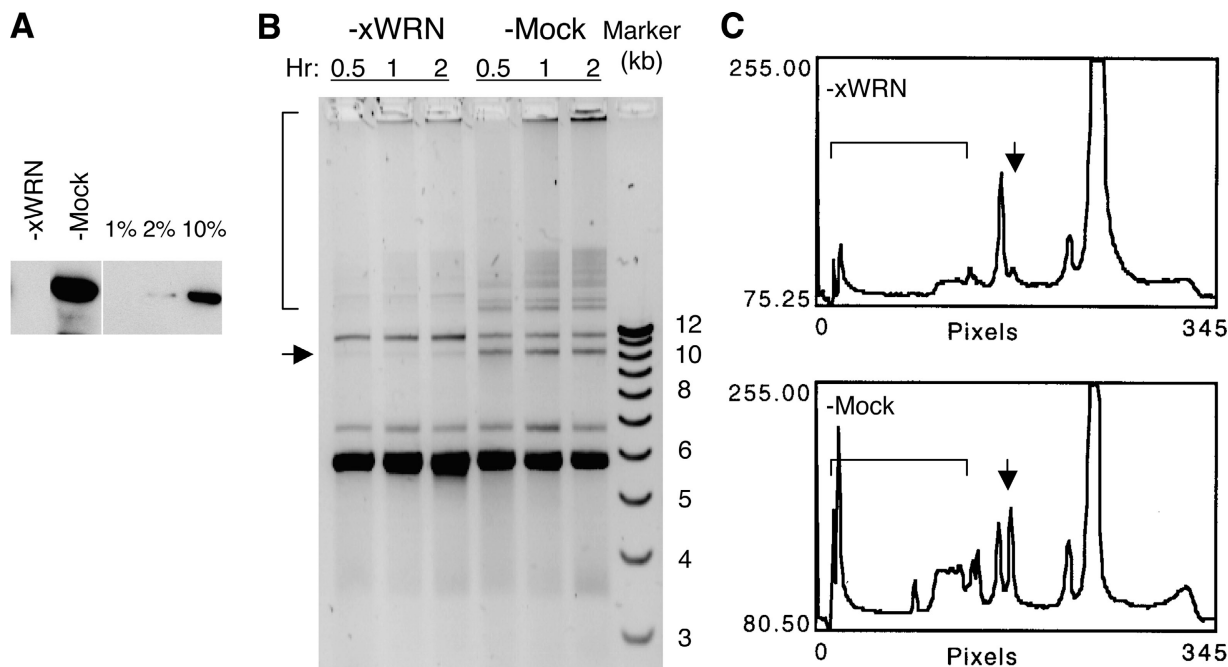


Figure 6. **Depletion of xWRN reduces SSA.** (A) Western blot of the depleted NPE. The three lanes on the right are quantitation controls and contain normal NPE at 1%, 2%, and 10% of the amount loaded in the lanes containing the depleted NPE. (B) SSA assay with xWRN-depleted and mock-depleted NPE. pRW4' was incubated in NPE for the indicated times, treated with SDS/proteinase K, and separated by agarose gel electrophoresis. The SSA products include the band indicated by the arrow and a subset of the bands indicated by the bracket. (C) Staining intensity plot of the lanes containing the 2-h repair products in (B).

XWRN is important for SSA

With the establishment of the SSA assay, we proceeded to determine if xWRN is important for this DSB repair pathway. xWRN was depleted from NPE with anti-xWRN antibodies to an undetectable level as judged by Western blot analysis (>98%) (Fig. 6 A). The depleted NPE was incubated with linear pRW4 (pRW4') as described in Fig. 3, and the repair products were separated by agarose gel electrophoresis. As shown in Fig. 6 B, the SSA products (indicated by arrow and bracket) were reduced significantly in xWRN-depleted NPE. Quantification of band intensity showed that the residual SSA products were <10% of those in the mock-depleted NPE. In contrast to the SSA products, the NHEJ products were not reduced, but increased slightly. The experiment in Fig. 2 showed that xWRN depletion did not affect NHEJ. A possible simple explanation for the increase in NHEJ in this experiment is that the ends were no longer channeled into SSA, and thus more of them were available for NHEJ. The differential effect on SSA and NHEJ indicated that the extract was not inactivated nonspecifically by the depletion procedure.

To determine if the inhibitory effect of xWRN depletion on SSA was specific, the xWRN protein that was purified from *Xenopus* cytosol (Fig. 7 A) was added back to the xWRN-depleted NPE. The purification procedure for xWRN involved multiple types of chromatography resins, but not anti-xWRN antibodies (Yan et al., 1998). As shown in Fig. 7, B and C, the addition of this purified xWRN led to a significant rescue of SSA. These results strongly suggest that xWRN is important for the SSA pathway of DSB repair.

Discussion

WRN has been implicated in DSB repair, but it is unclear if it does so directly or indirectly—and, if directly—in which DSB repair pathway. In this study, we analyzed systematically the role of xWRN in DSB repair. By using restriction enzymes to introduce DSBs into chromatin, we demonstrated that xWRN is recruited to DSB foci. These foci also contain the eukaryotic single-strand DNA binding protein, RPA. Previously, it was shown that RPA is associated with sequences close to DNA ends (Grandi et al., 2001), and that xWRN interacts physically and functionally with RPA (Chen et al., 2001). Therefore, it is reasonable to conclude that xWRN is associated with DNA ends. However, the DSB foci are distinct from replication foci that also contain xWRN and RPA. Whereas DSB foci contain DNA end-binding protein, Ku, but not replication initiation protein, CDC45, replication foci contain CDC45, but not Ku. These observations are consistent with the idea that xWRN has a dual function, one in replication and one in DSB repair.

To determine in which DSB repair pathway xWRN participates, we reconstituted SSA in NPEs. Previously, Carroll (1996) demonstrated that SSA is the major homology-dependent DSB repair pathway when DNA with homologous ends is injected into *Xenopus* oocytes and eggs. They also delineated the major steps in the SSA pathway: 5' → 3' end processing, annealing of complementary strands, processing of flaps, and ligation. This model is in agreement with the results that were derived from yeast genetic analysis of SSA repair (Ivanov et

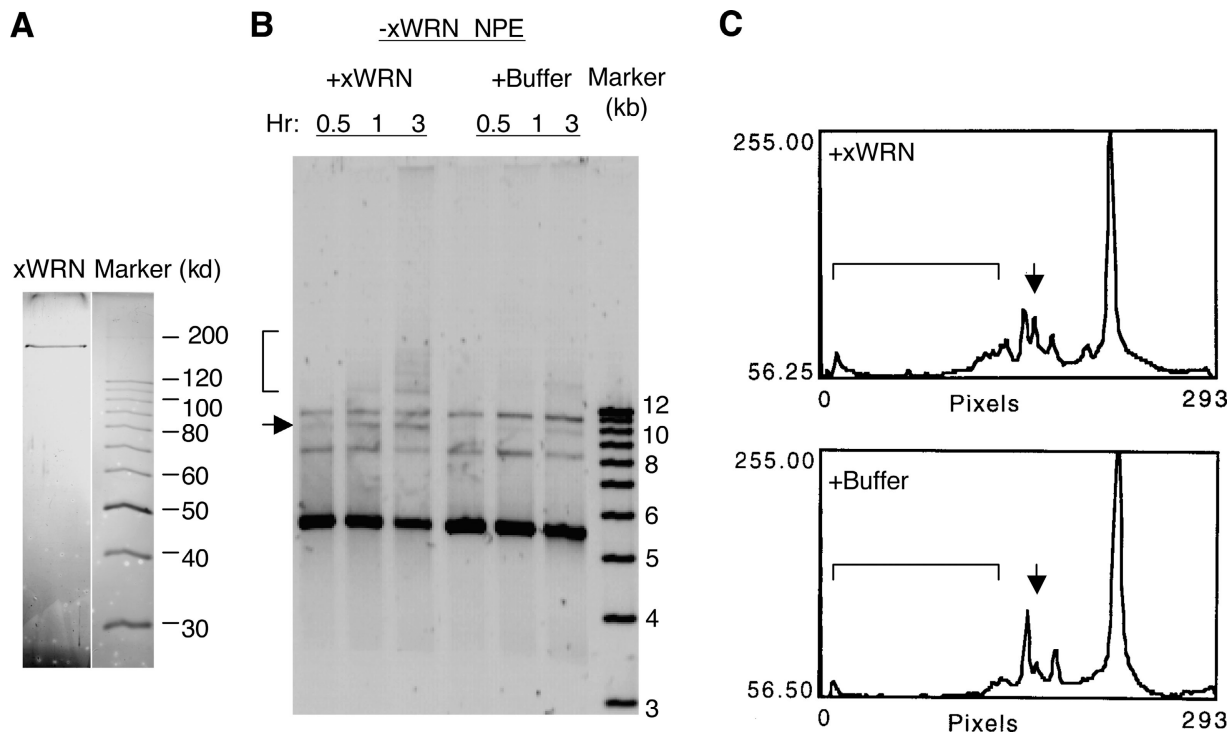


Figure 7. **Rescue of SSA by the xWRN protein.** (A) Silver staining of the xWRN protein purified from *Xenopus* egg cytosol by conventional column chromatography (Yan et al., 1998). (B) Add-back of purified xWRN to the xWRN-depleted NPE. pRW4' was incubated in xWRN-depleted NPE supplemented with xWRN (5 ng/ μ l final concentration) or buffer (ELB) for the indicated times and then analyzed by agarose gel electrophoresis. The SSA products include the band indicated by the arrow and a subset of the bands in the bracketed area. (C) Staining intensity plot of the lanes containing the 3-h repair products in (B).

al., 1996). The homology-based repair that we reconstituted in NPE depends on the homology being located at ends, and the repair product retains only one of the two repeats. It is distinct from NHEJ in that it is insensitive to dideoxynucleotides, whereas NHEJ is inhibited by these chain-terminating nucleotide analogs. In addition, it is independent of RAD51, the central protein that mediates strand invasion during HR. In *S. cerevisiae*, SSA also is independent of RAD51 function (Ivanov et al., 1996). Therefore, these features strongly suggest that the homology-based DSB repair pathway in NPE is SSA rather than HR.

One unique feature of the SSA reaction in NPE is that it is almost exclusively intermolecular. Intramolecular SSA would produce the circular pBR322 DNA, which were detected occasionally, but at extremely low levels (unpublished data). In fact, the intermolecular SSA is so efficient that, if NHEJ is blocked by ddNTP at the ends, SSA will continue to link more DNA molecules and lead to the formation of DNA that is too large to enter the agarose gel (Fig. 4). The preference for intermolecular reaction is not the intrinsic property of the DNA substrate used because NHEJ occurs almost equally efficiently by inter- and intramolecular mechanisms. One possible explanation is that the annealing step of SSA might depend on the proper alignment of the two long single strands. A 5.6-kb molecule, especially after nucleosomes are assembled on it, might not be long enough for the two single-strand tails to be aligned properly for efficient annealing. In contrast, NHEJ might require just the two ends to be juxtaposed, and as such, may not be as sensitive to the length of substrate DNA. In any event, the intermolecular nature better reflects the *in vivo* situation where the two repeats also are present on two different molecules after a break occurs between them.

Using the NPE SSA system, we determined the effect of xWRN depletion on SSA. The results clearly showed that xWRN is important for SSA. This is the first SSA protein to be identified by biochemical, rather than genetic, methods. Studies in yeast identified RAD52, RAD59, ERCC1, and MSH2 as being important for SSA (Paques and Haber, 1997; Sugawara et al., 2000). The yeast RecQ gene, SGS1, also is involved in SSA by rejecting heteroduplex formation (Sugawara et al., 2004). Human WS cells are defective in homology-dependent repair as assayed by recombination between two tandem direct repeat sequences (Prince et al., 2001). Previous studies showed that recombination events between direct repeats in this kind of assay occur by way of HR and SSA (Liang et al., 1998). As such, the results from our biochemical studies are consistent with the homology-dependent repair defect of WS cells. WRN is concentrated in nucleoli of human cells (Gray et al., 1998) and *Xenopus* cells (unpublished data), which contain ~200 copies of ribosomal gene repeats. Conceivably, WRN might participate in rDNA repeat repair by way of SSA in the nucleoli.

It remains to be determined how WRN might participate in SSA. WRN is endowed with a 3'→5' helicase activity and a 3'→5' exonuclease activity. The first step of homology-based repair (for SSA and HR) is the end processing to generate single-stranded DNA. However, the directionality of this end processing is 5'→3'. Thus, it is extremely unlikely that WRN is

the protein that directly performs end processing. However, end processing may be performed by the combined action of a DNA helicase and a nuclease (Symington, 2002), so it remains possible that WRN participates indirectly in end processing by promoting the unwinding of DNA ends. Another potential role for WRN in SSA is in the repair of the annealed single strands. WRN might act with FEN1, which is known to interact with WRN (Brosh et al., 2001), to excise the 5' flap that is left behind by incomplete end processing. Alternatively, WRN might act with DNA polymerase δ and PCNA, both of which interact with WRN (Kamath-Loeb et al., 2000; Lebel et al., 1999), to carry out the fill-in of the gaps (caused by excessive end processing) in the annealed DNA. Further experiments using the biochemical SSA assay described herein should answer these important mechanistic questions.

In contrast to SSA, we found no significant effect of xWRN depletion on NHEJ. Superficially, this result is in contradiction to the report that linear DNA suffers more end deletions after being introduced into WS cells (Oshima et al., 2002). However, it should be emphasized that WS and WRN knockout mice have no defect in V(D)J recombination (Lebel and Leder, 1998; Schellenberg et al., 1998), and as such, WRN is not an essential component of the NHEJ pathway. The end deletions in WS cells are more compatible with the idea that WRN indirectly modulates NHEJ by protecting ends from degradation. If NHEJ is the rate-limiting step for the repair of large quantities of linear DNA in WS cells, then the protective effect of WRN would be significant. In contrast, NHEJ is extremely efficient in *Xenopus* egg extracts; as such, the protective effect of xWRN may be insignificant. An alternative role for WRN in NHEJ is that it is recruited by Ku to degrade lesions at ends (Orren et al., 2001).

Approximately 50% of the human genome is made up of repetitive elements, such as Alu repeats, rDNA repeats, and centromeric repeats (Lander et al., 2001). Therefore, the probability of a DSB occurring in a repeat element is not insignificant. SSA and HR are competing homology-based pathways for the repair of such DSBs, and the choice of which repair pathway to use seems to be under cellular control (Wu et al., 1997; Liang et al., 1998). For example, mutations in BRCA2 cause a reduction of HR, but a stimulation of SSA (Tutt et al., 2001; Larminat et al., 2002). Although SSA generally is considered to be error-prone, whereas HR is considered to be error-free, in many situations, SSA may be less risky to genome integrity than HR. This is dictated by the differing mechanisms of the two homology-based repair processes. HR involves homology search; however, if the break is in a repeat, homology search would have many potential targets throughout the genome, and the missing information might be copied from the wrong repeat. There also is the risk of chromosome translocation if HR between repeats on different chromosomes proceeds by the Holliday junction-resolution mechanism. In contrast, SSA would be limited to the breakage point (unless there is a simultaneous second break elsewhere in the genome). Even if one of the repeats is deleted, the whole chromosome maintains the same linearity. Because the vast majority of the human genome is made of noncoding sequences, such deletions are unlikely to be detrimental to cells. Further studies of SSA using the NPE system would lead to a more com-

plete understanding of the intricate network that maintains genome stability in eukaryotic cells. In addition, based on the many features that are shared by SSA and HR, it is expected that these biochemical studies would also provide important mechanistic insights into mitotic HR.

Materials and methods

Extract preparation and nuclear reconstitution

Crude interphase *Xenopus* egg extracts, membrane-free cytosol, membrane, and demembrated sperm chromatin were prepared following the published procedures (Smythe and Newport, 1991). Nuclei for immunofluorescence staining were reconstituted at room temperature by mixing cytosol (1/3 volume), membrane (1/10 volume), and ATP-regeneration system/sperm chromatin cocktail (1/10 volume; 20 mM ATP, 200 mM phosphocreatine, 0.5 mg/ml creatine kinase, and 10,000/μl sperm chromatids). Egg lysis buffer (ELB; 10 mM Hepes [pH 7.5], 250 mM sucrose, 2.5 mM MgCl₂, 50 mM KCl, 1 mM DTT) was used to make up the rest of the volume. Nucleoplasmic extracts (NPEs) were prepared exactly following the published protocol (Walter et al., 1998).

Antibody preparation

The following antibodies were used in this study: rat anti-RPA (p70 subunit of *Xenopus* RPA), rabbit anti-xWRN (amino acids 1032–1436), and rabbit anti-xRAD51. The antibodies were raised against the gel-purified recombinant GST fusion proteins, according to the standard procedure (Goding, 1986). They were purified by passing the sera through affinity columns that were constructed with the corresponding fusion proteins, following the procedure that was described previously (Yan et al., 1993). The bound antibodies were eluted with 50 mM glycine (pH 2.5) and then renatured rapidly with 1/10th volume of 1 M Tris-HCl (pH 8). Anti-GST antibodies were removed by another affinity column that was constructed with the GST protein.

Indirect immunofluorescence staining

Indirect immunofluorescence staining was performed as described before (Yan and Newport, 1995). In brief, samples were fixed with equal volumes of fixation solution (3% formaldehyde/2% sucrose in PBS). After 10 min, nuclei were spun through 1 M sucrose/PBS onto coverslips and then treated with 0.1% Triton X-100/PBS for 5 min. The coverslips were blocked with 10% FCS for 20 min and then stained with the appropriate primary and secondary antibodies. Secondary antibodies were goat anti-rat FITC and goat anti-rabbit TR (The Jackson Laboratory). Images were collected with a monochrome DAGE-MTI cooled CCD-300-RT camera under the control of Scion Image 1.6.1 (Scion Corp.) and processed in Photoshop 5.5 (Adobe Systems).

Immunodepletion

Immunodepletion of cytosol was performed by incubating cytosol (40 μl + 20 μl ELB) with 20 μl Protein A Sepharose beads (GE Healthcare) that had been pre-coated with 4 μg of the affinity-purified rabbit anti-xWRN antibodies or rabbit IgG. After incubation at 4°C for 2.5 h, the beads were removed by low-speed centrifugation and the supernatants were incubated again with a fresh batch of antibody-coated beads. Immunodepletion of NPE (for xWRN and xRAD51) was performed by a similar procedure, except that 16 μg antibodies were used for 40 μl NPE (diluted to 60 μl with ELB). Because of the difficulty in preparing good quality NPE and depleting xWRN from it, depleted NPE was reserved exclusively for SSA experiments. NHEJ experiments were conducted in cytosol, which is fully competent for this reaction, but not for SSA.

NHEJ assay

The substrates for the NHEJ assay were prepared by digesting plasmid pUC19 with restriction enzymes to create various combinations of ends: BamHI/HincII for 5'/blunt, KpnI/HincII for 3'/blunt, and BamHI/PstI for 5'/3'. The NHEJ reactions contained 0.5 μl 10x ATP mix (20 mM ATP + 0.2 M creatine phosphate + 0.5 mg/ml phosphocreatine kinase), 5 μl depleted cytosol, and 0.5 μl DNA at the indicated concentrations. The reactions were incubated at room temperature for 2 h. For gel electrophoresis analysis, 2-μl samples were incubated with 2 μl 2x sample buffer (80 mM Tris-HCl [pH 8], 0.13% phosphoric acid, 8 mM EDTA, 5% SDS, 0.2% bromophenol blue, and 10% Ficoll) and 0.5 μl proteinase K (10 mg/ml in H₂O) at room temperature for ≥2 h, and then separated on 1% Tris acetic

acid EDTA/agarose gels. For sequencing the repaired junctions, DNA was purified after 2 h of incubation by QIAGEN PCR purification column, and used for transformation into *E. coli* strain DH5α. Plasmid DNA was isolated from individual colonies and the junctions were sequenced.

SSA assay

The substrates for the SSA assays were prepared from plasmid pRW4, which carries a 1.2-kb direct repeat of the tetracycline resistance gene (*Tet*) (Maryon and Carroll, 1989). The DNA was linearized by the restriction enzyme *Xho*I, which has a unique site between the two *Tet* repeats. The ends were filled in partially with TTP and dCTP to prevent simple religation. In the experiment of Fig. 5, another plasmid, pACYC184 (New England Biolabs, Inc.), was digested with *Cla*I and *Xba*I or with *Nco*I to place the *Tet* gene at the end or in the middle, respectively. In addition, in this experiment, the pRW4 ends were partially filled in with TTP, dCTP, and ddGTP, and the pACYC184 ends were partially filled in with TTP, dATP, dCTP, and ddGTP. A typical SSA assay contained 0.5 μl 10x ATP mix, 5 μl NPE (either 2.5 μl normal NPE + 2.5 μl ELB buffer or 5 μl depleted NPE), and 12 ng/μl DNA in a 6-μl reaction. For complementation, 0.5 μl purified xWRN or ELB buffer was included in the reaction. After incubation at room temperature, 2-μl samples were taken out at the indicated times and mixed with 2 μl 2x sample buffer and 0.5 μl proteinase K. After incubation at room temperature for ≥2 h, the samples were separated on 1% Tris acetic acid EDTA/agarose gels. The junction region in the 10-kb repair product was amplified with primers 5'-GTGCCACCT-GACGTCTAAG-3' and 5'-AGATGGCGGACGCGATGG-3' that bracket the *Tet* gene.

Online supplemental material

Fig. S1 shows alignment between the junction sequence of an SSA clone and pBR322 (New England Biolabs, Inc.). Fig. S2 shows alignment between the sequence of the PCR-amplified junction and pBR322. Online supplemental material available at <http://www.jcb.org/cgi/content/full/jcb.200502077/DC1>.

The authors thank Dr. D. Carroll for providing the pRW4 plasmid, and Drs. A. Skalka and Y. Matsumoto for reading the manuscript before submission.

This research was supported by grants from the V Foundation, Ellison Medical Foundation, and National Institutes of Health (R01 GM57962-02) to H. Yan.

Submitted: 11 February 2005

Accepted: 19 September 2005

References

- Baumann, P., and S.C. West. 1998. Role of the human RAD51 protein in homologous recombination and double-strand-break repair. *Trends Biochem. Sci.* 23:247–251.
- Blander, G., N. Zalle, Y. Daniely, J. Taplick, M.D. Gray, and M. Oren. 2002. DNA damage-induced translocation of the Werner helicase is regulated by acetylation. *J. Biol. Chem.* 277:50934–50940.
- Brosh, R.M., Jr., C. von Kobbe, J.A. Sommers, P. Karmakar, P.L. Opreško, J. Piotrowski, I. Dianova, G.L. Dianov, and V.A. Bohr. 2001. Werner syndrome protein interacts with human flap endonuclease 1 and stimulates its cleavage activity. *EMBO J.* 20:5791–5801.
- Carroll, D. 1996. Homologous genetic recombination in *Xenopus*: mechanism and implications for gene manipulation. *Prog. Nucleic Acid Res. Mol. Biol.* 54:101–125.
- Chen, C.Y., J. Graham, and H. Yan. 2001. Evidence for a replication function of ffa-1, the *xenopus* orthologue of Werner syndrome protein. *J. Cell Biol.* 152:985–996.
- Comai, L., and B. Li. 2004. The Werner syndrome protein at the crossroads of DNA repair and apoptosis. *Mech. Ageing Dev.* 125:521–528.
- Constantinou, A., M. Tarsounas, J.K. Karow, R.M. Brosh, V.A. Bohr, I.D. Hickson, and S.C. West. 2000. Werner's syndrome protein (WRN) migrates Holliday junctions and co-localizes with RPA upon replication arrest. *EMBO Rep.* 1:80–84.
- Cooper, M.P., A. Machwe, D.K. Orren, R.M. Brosh, D. Ramsden, and V.A. Bohr. 2000. Ku complex interacts with and stimulates the Werner protein. *Genes Dev.* 14:907–912.
- Cox, M.M., M.F. Goodman, K.N. Kreuzer, D.J. Sherratt, S.J. Sandler, and K.J. Marians. 2000. The importance of repairing stalled replication forks. *Nature.* 404:37–41.
- Crabbe, L., R.E. Verdun, C.I. Hagglom, and J. Karlseder. 2004. Defective telo-

- mere lagging strand synthesis in cells lacking WRN helicase activity. *Science*. 306:1951–1953.
- Fujiwara, Y., T. Higashikawa, and M. Tatsumi. 1977. A retarded rate of DNA replication and normal level of DNA repair in Werner's syndrome fibroblasts in culture. *J. Cell. Physiol.* 92:365–374.
- Fujiwara, Y., Y. Kano, M. Ichihashi, Y. Nakao, and T. Matsumura. 1985. Abnormal fibroblast aging and DNA replication in the Werner syndrome. *Adv. Exp. Med. Biol.* 190:459–477.
- Fukuchi, K., G.M. Martin, and R.J. Monnat Jr. 1989. Mutator phenotype of Werner syndrome is characterized by extensive deletions. *Proc. Natl. Acad. Sci. USA*. 86:5893–5897 (published erratum appears in Proc Natl Acad Sci USA 1989 Oct;86(20):7994).
- Fukuchi, K., K. Tanaka, Y. Kumahara, K. Marumo, M.B. Pride, G.M. Martin, and R.J. Monnat Jr. 1990. Increased frequency of 6-thioguanine-resistant peripheral blood lymphocytes in Werner syndrome patients. *Hum. Genet.* 84:249–252.
- Goding, G.W. 1986. *Monoclonal Antibodies: Principles and Practice*. Academic Press, New York. 315 pp.
- Grandi, P., E. Michail, I. Nielsen, and I. Raska. 2001. DNA double-strand breaks induce formation of RP-A/Ku foci on in vitro reconstituted *Xenopus* sperm nuclei. *J. Cell Sci.* 114:3345–3357.
- Gray, M.D., L. Wang, H. Youssoufian, G.M. Martin, and J. Oshima. 1998. Werner helicase is localized to transcriptionally active nucleoli of cycling cells. *Exp. Cell Res.* 242:487–494.
- Hanaoka, F., F. Takeuchi, T. Matsumura, M. Goto, T. Miyamoto, and M. Yamada. 1983. Decrease in the average size of replicons in a Werner syndrome cell line by Simian virus 40 infection. *Exp. Cell Res.* 144:463–467.
- Hoehn, H., E.M. Bryant, K. Au, T.H. Norwood, H. Boman, and G.M. Martin. 1975. Variegated translocation mosaicism in human skin fibroblast cultures. *Cytogenet. Cell Genet.* 15:282–298.
- Ivanov, E.L., N. Sugawara, J. Fishman-Lobell, and J.E. Haber. 1996. Genetic requirements for the single-strand annealing pathway of double-strand break repair in *Saccharomyces cerevisiae*. *Genetics*. 142:693–704.
- Kamath-Loeb, A.S., E. Johansson, P.M. Burgers, and L.A. Loeb. 2000. Functional interaction between the Werner syndrome protein and DNA polymerase delta. *Proc. Natl. Acad. Sci. USA*. 97:4603–4608.
- Khakhar, R.R., J.A. Cobb, L. Bjergbaek, I.D. Hickson, and S.M. Gasser. 2003. RecQ helicases: multiple roles in genome maintenance. *Trends Cell Biol.* 13:493–501.
- Kobayashi, T., S. Tada, T. Tsuyama, H. Murofushi, M. Seki, and T. Enomoto. 2002. Focus-formation of replication protein A, activation of checkpoint system and DNA repair synthesis induced by DNA double-strand breaks in *Xenopus* egg extract. *J. Cell Sci.* 115:3159–3169.
- Labhart, P. 1999. Ku-dependent nonhomologous DNA end joining in *Xenopus* egg extracts. *Mol. Cell. Biol.* 19:2585–2593.
- Lander, E.S., L.M. Linton, B. Birren, C. Nusbaum, M.C. Zody, J. Baldwin, K. Devon, K. Dewar, M. Doyle, W. FitzHugh, et al. 2001. Initial sequencing and analysis of the human genome. *Nature*. 409:860–921.
- Larminat, F., M. Germanier, E. Papouli, and M. Defais. 2002. Deficiency in BRCA2 leads to increase in non-conservative homologous recombination. *Oncogene*. 21:5188–5192.
- Lebel, M., and P. Leder. 1998. A deletion within the murine Werner syndrome helicase induces sensitivity to inhibitors of topoisomerase and loss of cellular proliferative capacity. *Proc. Natl. Acad. Sci. USA*. 95:13097–13102.
- Lebel, M., E.A. Spillare, C.C. Harris, and P. Leder. 1999. The Werner syndrome gene product co-purifies with the DNA replication complex and interacts with PCNA and topoisomerase I. *J. Biol. Chem.* 274:37795–37799.
- Lee, J.W., J. Harrigan, P.L. Opresko, and V.A. Bohr. 2005. Pathways and functions of the Werner syndrome protein. *Mech. Ageing Dev.* 126:79–86.
- Li, B., and L. Comai. 2000. Functional interaction between Ku and the Werner syndrome protein in DNA end processing. *J. Biol. Chem.* 275:28349–28352.
- Liang, F., M. Han, P.J. Romanienko, and M. Jasin. 1998. Homology-directed repair is a major double-strand break repair pathway in mammalian cells. *Proc. Natl. Acad. Sci. USA*. 95:5172–5177.
- Lisby, M., J.H. Barlow, R.C. Burgess, and R. Rothstein. 2004. Choreography of the DNA damage response: spatiotemporal relationships among checkpoint and repair proteins. *Cell*. 118:699–713.
- Lohka, M.J., and Y. Masui. 1983. Formation in vitro of sperm pronuclei and mitotic chromosomes induced by amphibian ooplasmic components. *Science*. 220:719–721.
- Lopes, M., C. Cotta-Ramusino, A. Pelliccioli, G. Liberi, P. Plevani, M. Muzi-Falconi, C.S. Newlon, and M. Foiani. 2001. The DNA replication checkpoint response stabilizes stalled replication forks. *Nature*. 412:557–561.
- Martin, G.M., C.A. Sprague, and C.J. Epstein. 1970. Replicative life-span of cultivated human cells. Effects of donor's age, tissue, and genotype. *Lab. Invest.* 23:86–92.
- Maryon, E., and D. Carroll. 1989. Degradation of linear DNA by a strand-specific exonuclease activity in *Xenopus laevis* oocytes. *Mol. Cell. Biol.* 9:4862–4871.
- McGlynn, P., R.G. Lloyd, and K.J. Marians. 2001. Formation of Holliday junctions by regression of nascent DNA in intermediates containing stalled replication forks: RecG stimulates regression even when the DNA is negatively supercoiled. *Proc. Natl. Acad. Sci. USA*. 98:8235–8240.
- Mimura, S., and H. Takisawa. 1998. *Xenopus* Cdc45-dependent loading of DNA polymerase alpha onto chromatin under the control of S-phase Cdk. *EMBO J.* 17:5699–5707.
- Mushegian, A.R., D.E. Bassett Jr., M.S. Boguski, P. Bork, and E.V. Koonin. 1997. Positionally cloned human disease genes: patterns of evolutionary conservation and functional motifs. *Proc. Natl. Acad. Sci. USA*. 94:5831–5836.
- Newport, J. 1987. Nuclear reconstitution in vitro: stages of assembly around protein-free DNA. *Cell*. 48:205–217.
- Orren, D.K., A. Machwe, P. Karmakar, J. Piotrowski, M.P. Cooper, and V.A. Bohr. 2001. A functional interaction of Ku with Werner exonuclease facilitates digestion of damaged DNA. *Nucleic Acids Res.* 29:1926–1934.
- Oshima, J., S. Huang, C. Pae, J. Campisi, and R.H. Schiestl. 2002. Lack of WRN results in extensive deletion at nonhomologous joining ends. *Cancer Res.* 62:547–551.
- Paques, F., and J.E. Haber. 1997. Two pathways for removal of nonhomologous DNA ends during double-strand break repair in *Saccharomyces cerevisiae*. *Mol. Cell. Biol.* 17:6765–6771.
- Pfeiffer, P., and W. Vielmetter. 1988. Joining of nonhomologous DNA double strand breaks in vitro. *Nucleic Acids Res.* 16:907–924.
- Postow, L., C. Ullsperger, R.W. Keller, C. Bustamante, A.V. Vologodskii, and N.R. Cozzarelli. 2001. Positive torsional strain causes the formation of a four-way junction at replication forks. *J. Biol. Chem.* 276:2790–2796.
- Prince, P.R., M.J. Emond, and R.J. Monnat Jr. 2001. Loss of Werner syndrome protein function promotes aberrant mitotic recombination. *Genes Dev.* 15:933–938.
- Rodriguez-Lopez, A.M., D.A. Jackson, F. Iborra, and L.S. Cox. 2002. Asymmetry of DNA replication fork progression in Werner's syndrome. *Aging Cell*. 1:30–39.
- Sakamoto, S., K. Nishikawa, S.J. Heo, M. Goto, Y. Furuichi, and A. Shimamoto. 2001. Werner helicase relocates into nuclear foci in response to DNA damaging agents and co-localizes with RPA and Rad51. *Genes Cells*. 6:421–430.
- Salk, D., K. Au, H. Hoehn, and G.M. Martin. 1981. Cytogenetics of Werner's syndrome cultured skin fibroblasts: variegated translocation mosaicism. *Cytogenet. Cell Genet.* 30:92–107.
- Scappaticci, S., D. Cerimele, and M. Fraccaro. 1982. Clonal structural chromosomal rearrangements in primary fibroblast cultures and in lymphocytes of patients with Werner's syndrome. *Hum. Genet.* 62:16–24.
- Schellenberg, G.D., T. Miki, C.E. Yu, and J. Nakura. 1998. Werner syndrome. In *The Genetic Basis of Human Cancer*. Vol. 18. B. Vogelstein and K.W. Kinzler, editors. McGraw-Hill Inc., New York. 347–359.
- Shen, J.C., and L.A. Loeb. 2000. The Werner syndrome gene: the molecular basis of RecQ helicase-deficiency diseases. *Trends Genet.* 16:213–220.
- Smythe, C., and J.W. Newport. 1991. Systems for the study of nuclear assembly, DNA replication, and nuclear breakdown in *Xenopus laevis* egg extracts. *Methods Cell Biol.* 35:449–468.
- Sugawara, N., T. Goldfarb, B. Studamire, E. Alani, and J.E. Haber. 2004. Heteroduplex rejection during single-strand annealing requires Sgs1 helicase and mismatch repair proteins Msh2 and Msh6 but not Pms1. *Proc. Natl. Acad. Sci. USA*. 101:9315–9320.
- Sugawara, N., G. Ira, and J.E. Haber. 2000. DNA length dependence of the single-strand annealing pathway and the role of *Saccharomyces cerevisiae* RAD59 in double-strand break repair. *Mol. Cell. Biol.* 20:5300–5309.
- Symington, L.S. 2002. Role of RAD52 epistasis group genes in homologous recombination and double-strand break repair. *Microbiol. Mol. Biol. Rev.* 66:630–670.
- Takeuchi, F., F. Hanaoka, M. Goto, I. Akaoka, T. Hori, M. Yamada, and T. Miyamoto. 1982a. Altered frequency of initiation sites of DNA replication in Werner's syndrome cells. *Hum. Genet.* 60:365–368.
- Takeuchi, F., F. Hanaoka, M. Goto, M. Yamada, and T. Miyamoto. 1982b. Prolongation of S phase and whole cell cycle in Werner's syndrome fibroblasts. *Exp. Gerontol.* 17:473–480.
- Thode, S., A. Schafer, P. Pfeiffer, and W. Vielmetter. 1990. A novel pathway of DNA end-to-end joining. *Cell*. 60:921–928.
- Tutt, A., D. Bertwistle, J. Valentine, A. Gabriel, S. Swift, G. Ross, C. Griffin, J. Thacker, and A. Ashworth. 2001. Mutation in Brca2 stimulates error-prone homology-directed repair of DNA double-strand breaks occurring between repeated sequences. *EMBO J.* 20:4704–4716.

- Vilenchik, M.M., and A.G. Knudson. 2003. Endogenous DNA double-strand breaks: production, fidelity of repair, and induction of cancer. *Proc. Natl. Acad. Sci. USA*. 100:12871–12876.
- Walter, J., and J. Newport. 2000. Initiation of eukaryotic DNA replication: origin unwinding and sequential chromatin association of Cdc45, RPA, and DNA polymerase alpha. *Mol. Cell*. 5:617–627.
- Walter, J., L. Sun, and J. Newport. 1998. Regulated chromosomal DNA replication in the absence of a nucleus. *Mol. Cell*. 1:519–529.
- Wu, X., C. Wu, and J.E. Haber. 1997. Rules of donor preference in *Saccharomyces* mating-type gene switching revealed by a competition assay involving two types of recombination. *Genetics*. 147:399–407.
- Yan, H., C.Y. Chen, R. Kobayashi, and J. Newport. 1998. Replication focus-forming activity 1 and the Werner syndrome gene product. *Nat. Genet.* 19:375–378.
- Yan, H., A.M. Merchant, and B.K. Tye. 1993. Cell cycle-regulated nuclear localization of MCM2 and MCM3, which are required for the initiation of DNA synthesis at chromosomal replication origins in yeast. *Genes Dev.* 7:2149–2160.
- Yan, H., and J. Newport. 1995. An analysis of the regulation of DNA synthesis by cdk2, Cip1, and licensing factor. *J. Cell Biol.* 129:1–15.
- Yu, C.E., J. Oshima, Y.H. Fu, E.M. Wijsman, F. Hisama, R. Alisch, S. Matthews, J. Nakura, T. Miki, S. Ouais, et al. 1996. Positional cloning of the Werner's syndrome gene. *Science*. 272:258–262.